Ceramics International 50 (2024) 12828–12839

Contents lists available at ScienceDirect

Ceramics International

journal homepage: www.elsevier.com/locate/ceramint

Investigation on the effect of inorganic acid attack on composite prepared with MK-based geopolymer and waste cork dust

Giovanni Dal Poggetto **, Fabiana Altimari, Cristina Leonelli *, Luisa Barbieri

Department of Engineering "Enzo Ferrari", University of Modena and Reggio Emilia, Via P. Vivarelli 10, 41125, Modena, Italy

ARTICLE INFO

Handling Editor: Dr P. Vincenzini

Keywords:
Cork waste
Metakaolin
Alkali activation
Acid resistance
Microstructure
Mechanical performance

ABSTRACT

The chemical, microstructural and mechanical characterization of novel lightweight composites produced by adding waste cork dust to a metakaolin-based geopolymeric matrix prepared by alkaline activation is presented. The alkaline activator solutions used for the reticulation of the 3D aluminosilicate network at room temperature are composed of NaOH and sodium silicate to maintain a low cost of the final composite. In this line, the research of the highest addition of waste, e.g. cork dust, is pursued starting from 1 and reaching a maximum content of 10 wt% over metakaolin. The chemical stability is evaluated in water as well as in HNO_3 or in H_2SO_4 0.5 and 2.5 N solutions. The addition of cork does not affect the reticulation of the geopolymeric binder used as matrix, as is demonstrated by FT-IR and XRD analyses. The modification of the dense geopolymeric microstructure with the introduction of cork dust weakens the hardened composites that become more permeable to water and acid solutions increasing the weight loss after immersion and decreasing the mechanical resistance to compression. The mechanical performance of the hardened composite with 10 wt% of cork dust still seems to be sufficient for application as self-supporting thermal insulation panels. (195/200).

1. Introduction

Sustainable cements and, more generally, sustainable building materials have the dual advantage of reducing the CO_2 emissions compared to conventional cements while reusing a variety of inert inorganic materials, such as fly ash from power production plants or metallurgical slags [1]. A combination of different industrial by-products and residues/wastes is often proposed for lightweight construction elements or insulation panels. In the recent years, the thermal stability and flammability of cork [2] have accompanied its known chemical stability, extending its application from stoppers [3] to building materials [4–6].

Typically, organic base polymers have been used as matrix materials for composite insulation panels with a number of options to modify the hydrophilic character of the cork surface to achieve the hydrophobic character of the matrix [7,8]. Inorganic binders have also been tested as matrices to increase sustainability by eliminating the need for cork surface treatments. In addition, industrial residues or by-products such as slag or ceramic waste can be used as inorganic matrix materials that are hardened by alkali activation, avoiding the use of clinker as in ordinary Portland cement [9]. Sustainability could be enhanced if the cork used as filler or lightweight aggregate is sourced from an industrial cork waste stream [10]. When residues, especially when codified as waste, are used in manufacturing facilities, the control of emission, dusting or leaching should be carefully considered to avoid additional discomfort effects known as "Sick Building Syndrome" (SBS) [11]. It has been found that the main causes are related to chemical contaminants from indoor sources such as building materials, inadequate ventilation, excessive use of heating, ventilation and air conditioning (HVAC), and volatile organic compounds (VOCs) [12]. Insulating building materials when consolidated by alkali activation of inorganic matrices, rather than catalysed by organic solvents, play a relevant role in the SBS reduction thanks to the limited emission of pollutants within a building environment combined with a reduced use of HVAC.

In the literature it is possible to find several studies in which cork is used for the production of geopolymers or alkali-activated materials. There are studies that (i) evaluate the performance of geopolymers with cork additives at different granulations [13], (ii) study the influence of cork residues on metakaolin-zeolite-based geopolymers [14], (iii) consider the influence of cork additives in geopolymers on shielding properties enhanced by electromagnetic interference [15], (iv) evaluate

* Corresponding author.
** Corresponding author.
E-mail addresses: giovanni.dalpoggetto@unimore.it (G. Dal Poggetto), cristina.leonelli@unimore.it (C. Leonelli).

https://doi.org/10.1016/j.ceramint.2024.01.190
Received 1 November 2023; Received in revised form 4 January 2024; Accepted 13 January 2024
Available online 17 January 2024

the thermal and acoustic insulation performance of geopolymers or alkali-activated materials containing cork [16–18]. In addition, there are studies that confirm the thermal insulation capacity of cork embedded in lightweight materials such as panels, resin composites, textiles, mortars, concrete and bio-composites [19–23].

The present paper reports an experimental investigation of some innovative formulations of an inorganic matrix, i.e. alkali activated metakaolin, added with a cork dust derived from an industrial process to produce a composite material with a view to a possible application in insulating panels. The cork dust is an industrial by-product, and it has been used as received. In addition, the entire activation process is kept as sustainable as possible by using Na-based reactants as activator solutions and curing the resulting composites at room temperature. In this study, we focused on the chemical characterization of the cork residue used as filler and the overall chemical stability and durability of the final hardened composite, while in a previous paper we reported the thermo-mechanical properties of similar compositions [10]. In the present work, we present the chemical stability in water as well as in acid solutions of similar composites as an additional assessment of the optimal reticulation of the geopolymeric matrix, previously investigated by FT-IR and XRD. Another reason for studying the durability of geopolymeric materials in acidic environments is the possibility of exposing the lightweight insulation materials outdoors or inside buildings. Finally, the mechanical performance of the hardened composites before and after acid immersion was combined with microstructure characterization (density and SEM + EDS).

2. Materials and methods

2.1. Materials

In this study, we used ARGICAL™ M1000 metakaolin (MK), sourced from Imerys in France. The chemical composition of this MK, as reported by the manufacturer, includes: $SiO_2 = 55$; $Al_2O_3 = 40$, $Fe_2O_3 = 1.4$; $TiO_2 = 1.5$; $Na_2O + K_2O = 0.8$; $CaO + MgO = 0.3$; LOI = 1 (wt%). We also considered cork waste obtained from the production of agglomerated cork bottle closures by a local company (Italsughero dei F.lli Correggi S. r.l., Montecchio Emilia (RE), Italy). This cork waste, CW, is specifically generated during the smoothing phase of agglomerated cork caps and is collected directly through a cyclonic air filtration system. The cork dust consists of particles with a diameter distribution in the range 0.063 mm < diameter <1 mm. It contains polyurethane adhesive and paraffin, which are industrially used as binders and additives for cork particles, respectively. A more detailed characterization of this cork waste can be found in a previous work [24]. To prepare the NaOH solution, laboratory grade granules (96 wt%, Sigma Aldrich, Italy) were dissolved in deionized water to obtain a concentration of 8 M. In addition, a commercial sodium silicate solution (Ingessil, Verona, Italy) with a SiO_2/Na_2O molar ratio of 3.00, $SiO_2 = 26.50$ wt%, $Na_2O = 8.70$ wt%, pH = 11.7, density = 1.34 g/cm^3 at 20 °C, was used to formulate the geopolymers.

Acid solutions of different concentrations were prepared using HNO_3 65 wt%, (Sigma Aldrich, Italy) and H_2SO_4 96 wt%, (Carlo Erba, Italy).

2.2. Preparations of samples and acid solutions

To prepare the reference geopolymer formulation, as already optimized in previous works [10,25,26] and denoted as GP0, we mixed a given amount of dry metakaolin powder with an alkali solution (8 M NaOH and Na-silicate solution in a 1:1 ratio) under mechanical stirring. We then introduced increasing amounts of cork powder, specifically 2, 5, 7 and 10 % by weight based on dry MK content, resulting in the geopolymer composites labeled as GP-2CW, GP-5CW, GP-7CW and GP-10CW, respectively (as shown in Table 1). Two additional geopolymer formulations were also prepared to test the effect of cork waste when it was introduced at different percentages (5 % and 10 % by weight) into the already prepared GP0 fresh (wet) paste already prepared, labeled 95GP0-5CW and 90GP0-10CW (see Table 1). This second type of preparation resulted in a lower workability of the mixture compared to the first addition, so that also in this case it was not possible to increase the amount of cork dust above 10 wt%.

Table 1
Geopolymer formulations (a: L/S = liquid (Na-silicate + NaOH) to solid (MK + CW) ratio; b: CW/matrix = cork waste dust to wet geopolymer paste (MK + NaOH + Na-Silicate) ratio).

Sample Label	MK [g]	NaOH [g]	Na-Silicate [g]	Cork Waste [g]	L/S [a] [wt/wt]	CW/matrix [b] [wt/wt]
GP0	100	38	40	0	7.8	0
GP-2CW	98	38	40	2	7.8	0.01
GP-5CW	95	36.5	38	5	7.45	0.03
GP-7CW	93	35.7	37.2	7	7.3	0.04
GP-10CW	90	34	36	10	7.0	0.06
95GP0-5CW	53	20	21	5	7.1	0.05
90GP0-10CW	51	19	20	10	6.4	0.11

All the fresh paste preparations were obtained by mechanically mixing the powders and the liquids using a planetary mixer (Aucma 1400W, Acuma CO., LTD., Shandong, China). The freshly prepared paste was poured into cubic molds of 25 × 25 × 25 mm^3. After eliminating any air bubbles with a vibrating table, the molds were carefully sealed, and the geopolymers were cured at room temperature under conditions of 100 % relative humidity. The silicone molds were opened after one day of curing. We generated a minimum of 10 samples for each formulation to ensure the reproducibility of results in both mechanical and acid resistance tests. Characterization of all samples was performed after 28 days of ageing, as indicated in the research plan (Fig. 1).

To prepare solutions of HNO_3 and H_2SO_4 at different concentrations, we first performed normality calculations due to the diprotic nature of the sulfuric acid. The HNO_3 solutions at 0.5 N (0.5 M, 3 wt%) and 2.5 N (2.5 M, approximately 15 wt%) were prepared by using a 65 wt% HNO_3 solution and adjusting the volumes of the initial acid added to deionized water (Milli-Q treatments). Similarly, for the H_2SO_4 solutions at 0.5 N (0.25 M, 3 wt%) and 2.5 N (1.25 M, 14 wt%), we started with a 96 wt% H_2SO_4 solution.

2.3. Characterization of the geopolymeric composites

The steps of the experimental procedure are shown in Fig. 1. The hardened composites were tested after 28 days of ageing at room temperature in contact with the laboratory atmosphere (relative humidity around 60–70 %). First, the reticulation of the geopolymer was characterised (2.3.1 to 2.3.3); then the microstructure of the composites and their physical, chemical and mechanical properties were studied (2.3.4 to 2.3.7).

2.3.1. Chemical stability in water

In order to evaluate the consolidation of the geopolymer paste in the presence of cork, its chemical stability in water after 28 days of ageing was studied using an integrity test reported in the literature [27]. Deionized water was added to the sample at a solid to water weight ratio ranging of 1:100, with a single dense sample varying between 2 and 3 g. After 24 h, the sample was removed from the water and its weight was measured after drying in acetone (3 h) and solvent evaporation at room temperature (with an additional 3 h).

2.3.2. FT-IR characterisation

With the aim to evaluate the geopolymerization, FT-IR analysis (Prestige21 Shimadzu spectrophotometer, Shimadzu Italia s.r.l., Milan, Italy equipped with a detector deuterated triglycine sulphate with

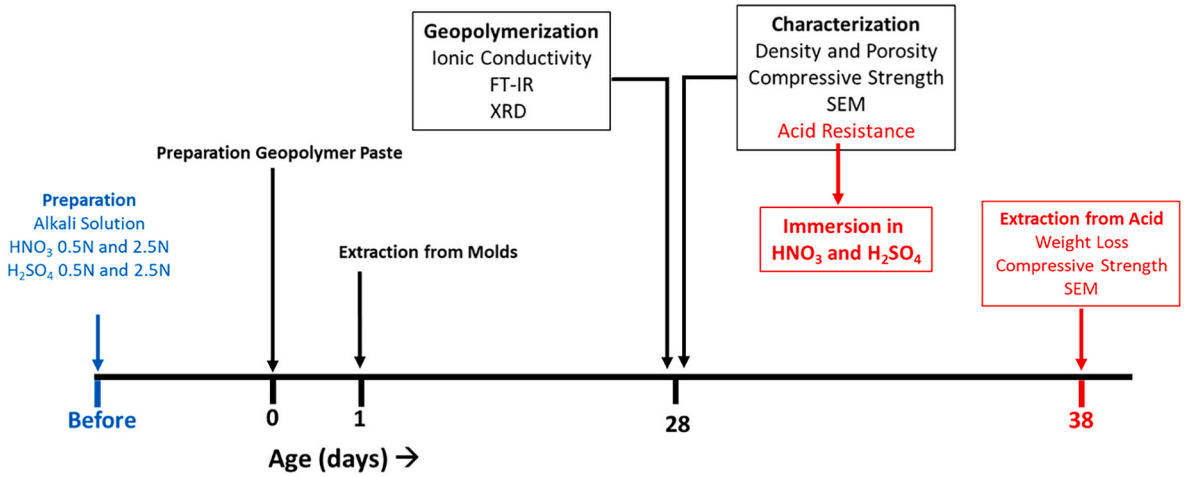

Fig. 1. Research plan on timeline.

potassium bromide windows) was performed on geopolymers with 10 wt% of CW added before and after the alkali activation and cork waste powder. The FT-IR analysis covered a range of 400–4000 cm^{-1} with a resolution of 2 cm^{-1}, and included 60 scans. For this analysis, we utilised KBr disks containing 2 mg of the sample and 198 mg of KBr. Subsequently, the FT-IR spectra were processed using IR-solution and Origin 9 software.

2.3.3. XRD characterisation

X-ray diffraction (XRD) analysis (X'Pert PRO, PANAlytical, Malvern Panalytical Ltd., Malvern, UK) was used to characterise the crystalline phases present in both the geopolymer formulation with 10 % of Cork waste. The X-ray diffractometer operated at 40 kV and 40 mA using Cu-Kα radiation (with Ni filtration). We collected diffraction patterns using the X'Celerator detector in the 2θ range from 5 to 70°, with a step size of 0.02° and a counting time of 3 s, and a slit width of 10. To identify mineral phases, we compared the experimental peaks with reference patterns using DIFFRAC plus EVA software (2005 PDF2, Bruker, Billerica, MA, USA). To ensure accurate results and to avoid preferential orientation, we applied a side loading to the powdered sample. Side loading of geopolymer powders for XRD measurements is critical, as has been shown in other publications [28,29], where preferential orientation can distort peak intensities and positions in the diffraction pattern, especially in phyllosilicates or phyllosilicate-derived structures.

2.3.4. Apparent density, real density and porosity

Apparent density, denoted as ρ_a, was determined geometrically by dividing the measured mass by the known volume of the cubic samples. To determine the average apparent density for each solidified composite, we computed the mean value from three separate measurements. Meanwhile, the real density, expressed as ρ_r, was determined using a helium pycnometer (Micromeritics Accupyc 1330, Micromeritics Instruments, Norcross, GA 30093, USA).

Using the real and apparent density values, the following equation was used to obtain the total porosity P% value:

$$P\% = (1-\rho_a/\rho_r)*1 \quad (1)$$

2.3.5. Chemical stability in acids

The study investigated the performance geopolymer in various acids by examining changes in appearance, mass, and compressive strength after 10 days according to modified ASTM C267 procedures. Geopolymer cubes were immersed in HNO_3 and H_2SO_4 solutions at concentrations of 0.5 N and 2.5 N. The cubes were exposed to the acid solutions while maintaining a constant of 8 between acid volume (in mL) and sample surface area (in cm^2) as described by Chang et al. [30]. After 10 days, the weight loss was determined by weighing the cubes after immersion. The samples were then washed with tap water, dried, and reweighed to calculate the percentage of weight loss. To measure the depth of acid infiltration into the geopolymers, a post-cracking test was conducted. A 1 % phenolphthalein solution was delicately sprayed on the specimens. Areas that retained their original white colour indicated acid infiltration, while purple areas retained geopolymeric alkalinity corresponding to the absence of an acid reaction. This colouration was instrumental in correctly sampling the portions of the bulky specimens to be examined in the SEM.

2.3.6. SEM observation

A SEM (ESEM-Quanta200-FEI) equipped with EDS (energy dispersive spectroscopy) was used to examine the microstructure of hardened samples after 28 days of curing. The purpose of this analysis was to evaluate the evolution of the geopolymeric amorphous phase and the presence of unreacted cork and aluminosilicate particles. To prepare for SEM analysis, a thin layer of gold was sputtered onto the freshly fractured surface of each specimen, which was accurately sampled after the acid attack using the phenolphthalein staining test.

2.3.7. Mechanical properties

After 28 days of curing, the mechanical properties of the cubic specimens were evaluated by compression testing using an Instron 5567 Universal Testing Machine. The load, limited to 30 kN, was applied incrementally at a displacement rate of 1 mm/min. The compressive strength values reported represent the average of eight tests with a variation of up to 2 %.

3. Results and discussion

3.1. Chemical stability in water

After ageing the geopolymers for 28 days, all samples were immersed in deionized H_2O for 24 h to observe the stability in water. It can be seen that the weight loss increases linearly with the percentage of cork waste when added together with MK before alkaline activation along (Fig. 2). The addition of CW seems to disrupt the reticulation of the geopolymer matrix. This could be due to the partial absorption of the activator solution by part of the cork dust, depriving the MK of its required proportion of reactant.

The linear trend is also similar when CW is added after alkali activation (95GP0-5CW and 90GP0-10CW), but the values at the same percentages differ from GP0 (Fig. 2). The addition of CW to the fresh

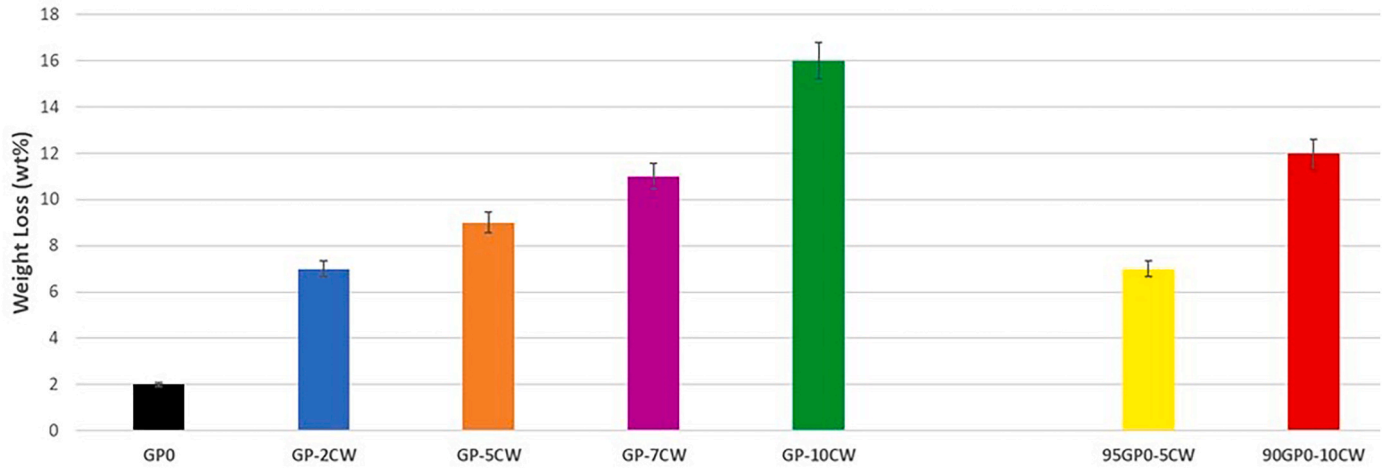

Fig. 2. Weight loss of all geopolymers after 24 h immersion in water (samples were aged for 28 days before test).

geopolymer paste, rather than to the dry MK, seems to less affect the weight loss in water and to produce a more stable composite in water, at least for 24 h of immersion. Consistent to what was assumed in the previous series of composites, in this case the cork dust was added to the already mixed geopolymeric paste, thus minimising the sequestration of alkaline activator from part of the cork dust.

Fig. 3 provides a comprehensive representation of the ionic conductivity values of the eluate after immersion in water of the composite samples, offering a comparative analysis against GP0. This data visualisation allows us to gain valuable insight into the impact of the presence of cork within the geopolymer matrix on the overall ionic conductivity of the eluate. The experimental results show a remarkable trend. When the waste cork (CW) is introduced into the metakaolin (MK) prior to the addition of the activator solution, the ionic conductivity values exhibit a distinct pattern. Specifically, as the proportion of cork in the mixture increases, there is a corresponding increment in ionic leaching with a corresponding increase in the measured ionic conductivity. This observation suggests that the incorporation of cork into the dry powders hinders the reticulation of the geopolymeric matrix and its release of ions into solution is high [31]. Conversely, when CW is incorporated into the sample as a filler with the primary purpose of reducing density or increasing lightness, the ionic conductivity values remain relatively low and close to that of the matrix (GP0). This consistency implies that the presence of cork does not significantly disrupt or alter the cross-linking and structure of the geopolymeric matrix, confirming the results of Fig. 2. Consequently, it can be concluded that the preparation process adopted for the samples 95GP0-5CW and 90GP0-10CW, where CW is added as a filler has the least effect on the chemical stability of the composite in water for a short period of time (24 h) compared to the process where cork dust is added to MK. This result highlights its potential utility in achieving lightweight geopolymer composites without compromising chemical properties.

3.2. FT-IR characterization

In the FT-IR spectrum of GP0 aged 28 days, the absorption bands appear very similar to those of composites containing cork dust. In particular, the samples with the highest cork content, 10 wt%, added before and after the alkali activation, show almost overlapping vibrational spectra (Fig. 4). Apart from the bands at 3440 cm^{-1} and 1650–1640 cm^{-1}, which are assigned to the stretching and bending modes of the –OH groups in water and cork cellulose [25,26,32], the spectra are dominated by a characteristic feature of the geopolymer matrix is the Si–O-T (T = Si, Al) band at about 1030 cm^{-1}. This peak is very important because it is used to follow the formation of geopolymer network, in fact this peak in the metakaolin powders is usually at 1080 cm^{-1} and this band shifts to a lower wavenumber (1030 and 1015 cm^{-1}) suggesting the increase of Si–O–Al bonds [33–35], especially for sample 90GP0-10CW. The introduction of Al into the Si–O–Si network brings a Na^{+} ion as a charge balance, thus reducing the amount of sodium leached during immersion in water (see Fig. 3).

Not clearly visible, but very interesting, is the shoulder positioned at about 870 cm^{-1}, which is assigned to the $Si–O^{-}$ non-bridging oxygen (NBO) stretching mode with one NBO involved per SiO_4 tetrahedron (Q3

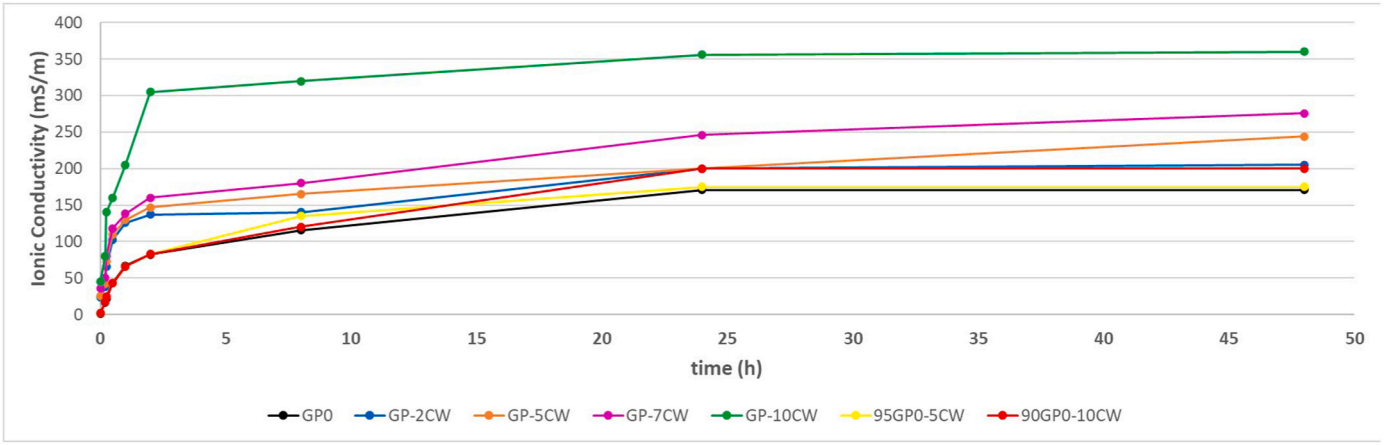

Fig. 3. Ionic conductivity of the water after immersion of all samples compared with GP0 (The reproducibility of the test was calculated to be within an error of 5 %).

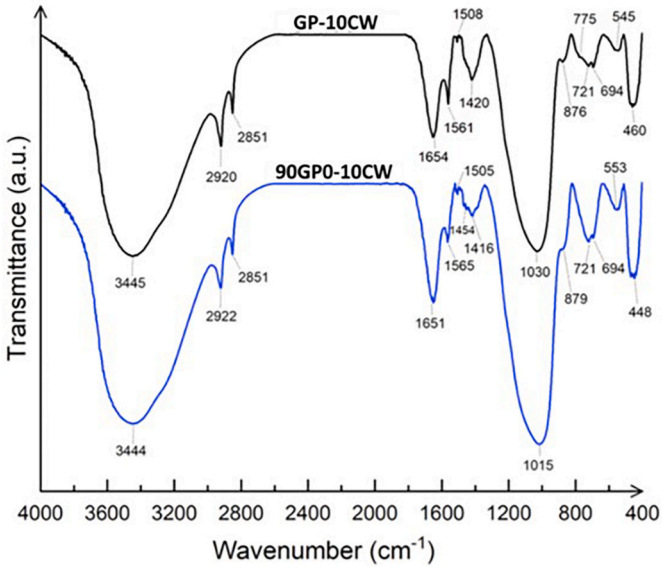

Fig. 4. FT-IR spectra of GP-10CW and 90GP0-10CW.

groups, requiring 3 bridging O and 1 NBO per SiO_4 tetrahedron) [36]. The presence of NBO can result from protonation of the siloxane bridges in acidic media, but also the presence of silanol groups, SiOH, are compatible with Q3 groups [37]. The peak detected at 800 cm^{-1}, attributed to Si–O bending [37], indicates the presence of quartz [25], while the band at 560 cm^{-1} is related to Al–O vibration in six-fold coordination [38,39]. The band at 470 cm^{-1} is assigned to the Si–OH bending mode [25]. In addition, the absorption band at 1420 cm^{-1} is attributed to carbonate stretching [40], and the bands at 470–450 cm^{-1} are ascribed to the Si–O–Si and O–Si–O bending modes [25,26,32].

The medium broad band at 474 cm^{-1} is attributed to Al–O vibrations, while the peaks around 450 cm^{-1} could be attributed to Fe–O vibrations [41]. Finally, Ti–O absorption broad bands are assigned around 430 cm^{-1} [41].

The distinctive features of cork manifest as peaks at 3400 cm^{-1} (indicative of the –OH bond), 2920 cm^{-1}, and 2850 cm^{-1} (representing stretching), along with a peak at 1737 cm^{-1} (indicative of bending) [24]. Paraffin content is discernible at 1459 cm^{-1} (reflecting bending) [42], while polyurethane glues can be identified by the peaks at 1235, 1156, and 1094 cm^{-1} (associated with bending), as well as at 721 cm^{-1} (indicative of bending-rocking) [24,43].

As can be seen (Fig. 4), the spectra are almost identical, allowing us to assert that the analysis of the vibrational spectra does not allow the definition of a significant distinction between the geopolymerization degree of the two different samples as fine as the ionic conductivity can do. At short range order, second or third coordination spheres around Si

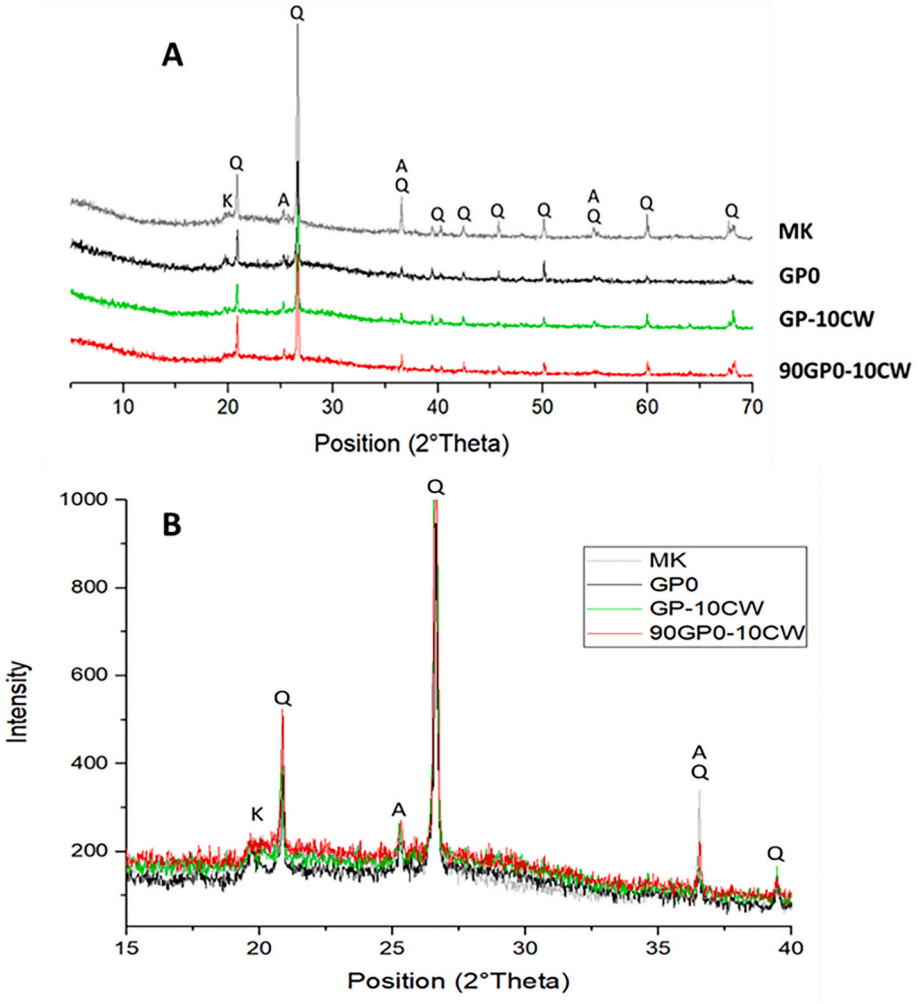

Fig. 5. XRD spectra of: A) GP-10CW and 90GP0-10CW compared with MK powder and MK-based geopolymer GP0; B) Enlargement of spectra A at the same intensity in the range 15–40° in 2 theta.

or Al, we can assess that the CW does not affect the geopolymerization.

3.3. XRD characterisation

Mineralogical analysis was performed on all samples (Fig. 5). Interestingly, the spectra of the remaining samples (GP-2CW, GP-5CW, GP-7CW, and 95GP0-5CW) mirrored those of the two spectra shown in Fig. 5a. The comparison focused exclusively on these two spectra due to their notably high cork content, indicating the likelihood of significant changes being evident in these specific samples.

In the diffraction pattern of GP0 (Fig. 5a), a diffuse reflection is clearly visible, indicating the typical broad band of the amorphous aluminosilicate structure. In addition, there are distinct sharper peaks identified as anatase and alpha-quartz. The diffraction patterns of all samples are similar and show these characteristic features. All three geopolymers exhibit diffuse reflections typical of an amorphous aluminosilicate network at about 26–28° in 2θ, with a slight shift toward higher values with respect to the position of the pristine metakaolin (Fig. 5b) [26,44]. In Fig. 5b, it can be seen that the characteristic peak of geopolymers between 20 and 35° remains unaffected, with no discernible shift attributed to the cork dust, whether added before or after alkali activation.

The XRD analysis can be considered as a qualitative approach to define the 3D aluminosilicate network of the geopolymer, which in this case shows three spectra that are almost identical, demonstrating that we cannot estimate any obvious change in the chemistry of the geopolymer by part of the cork.

3.4. Apparent density, real density and porosity

Fig. 6 shows the variation of apparent density, real density, and porosity as a function of cork percentage. Apparent density decreases as cork percentage increases for both series of cork-containing composites aged 28 days. Cork is a lightweight and inherently porous material that is very sensitive to moisture, causing the composite to become lighter [45].

A single wine cork stopper contains approximately 700 million cells, a result of the intricate cellular composition of the inner bark of the cork oak, which consists of independent tetra-decahedron cells. Even after processing, this cellular arrangement is maintained in cork stoppers [46].

The real density decreases as the percentage of cork increases over the 28 days, in accordance with the change in bulk density.

The evolution of total porosity (Fig. 6) mirrors the observations in Fig. 2, reflecting the corresponding water loss values; in addition, it is possible to see the evolution of the porosity over the 28 days of ageing. In particular, the sample with the highest addition of cork waste before alkali activation has an exceptionally high porosity value, around 35 %. When cork is added after alkaline activation, the porosity reaches up to 42 % for both compositions. It is crucial to note that metakaolin-based geopolymers inherently possess nano porosity in the range of 35–40 %, characterised by nano pores within the mesoporous scale (2–50 nm) [47]. The challenge arises from the complicated evaporation of condensation water through these ultrafine pores, which is exacerbated by the introduction of cork powder, accompanied by the formation of voids around it due to the difficult workability of the material in its fresh geopolymer paste state. The difficult workability may have affected the homogeneity of the samples and biased the porosity value in the sample containing 7 wt% cork, as the value is lower than in the 2 and 5 wt% additions.

The results obtained are in agreement with literature data [19], as the percentage of cork increases, the density of the composite decreases, resulting in a light and very porous material. Probably, the high porosity value allows obtaining a good insulator, as demonstrated by the authors in a previous work [10].

3.5. Chemical stability in acid

After preparing solutions of HNO_3 and H_2SO_4 at the two concentrations, 0.5 and 2.5 N, the samples were immersed for 10 days. Initially, the samples were immersed in the least concentrated solutions. As shown in Fig. 7 and detailed in the graph of the mechanical properties (see details in Fig. 13), the samples exhibited strong resistance to acid attack after 10 days. Subsequently, we immersed the samples in more concentrated acidic solutions, which produced significantly different results. The percentage loss increased dramatically as the CW addition increased, consistent with the porosity results.

Sulfuric acid has a slightly higher disruptive effect compared to nitric acid, but the concentration of the two acids is the main player, supporting the model of the depolymerization/degradation of aluminosilicate 3D network in acidic media reported in the literature [48–51]. In particular, the depolymerization process starts with the exchange of H^+ for Na^+, thus creating a number of new Al–O–H as well as Si–O–H bonds, which causes the loss of mass of part of the geopolymeric matrix. The

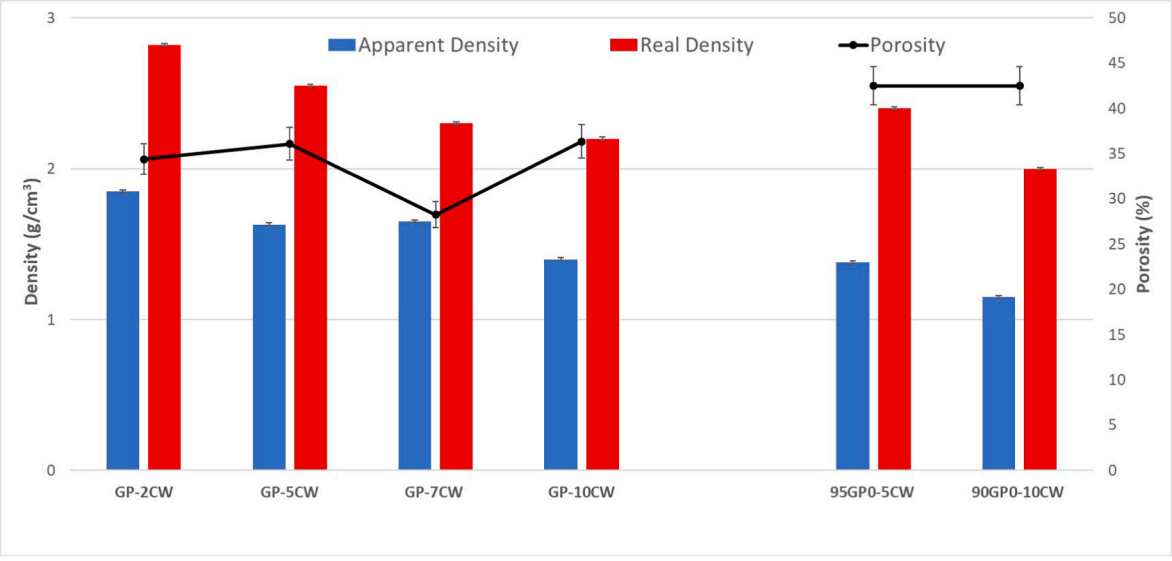

Fig. 6. Real density, apparent density and porosity of all geopolymers aged 28 days.

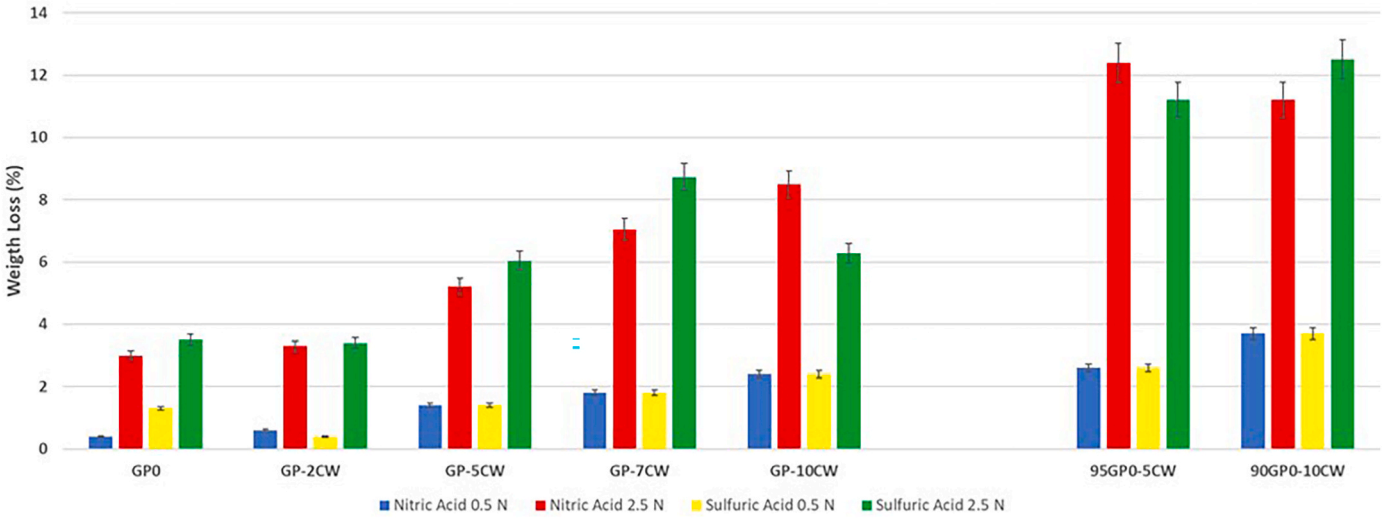

Fig. 7. Weight loss (%) of the 28 aged samples after additional 10 days of immersion in HNO_3 and H_2SO_4.

cork is almost unaffected by the acidic environment, as reported in the literature [52].

For samples 95GP0-5CW and 90GP0-10CW, the weight loss is higher than for the other series of samples. This chemical instability in acid can be correlated with the evolution of the porosity of these two samples (95GP0-5CW and 90GP0-10CW), which resulted to higher than the two corresponding GP-5CW and GP-10CW, rather than the total amount of cork (see also Fig. 6).

3.6. SEM observation

Fig. 8 presents the Scanning Electron Microscopy (SEM) image of cork waste showing its typical irregular surface structure, characterised by a network of small voids, pores, and grooves. The distinctive porous composition of cork, essential for its insulating properties, is evident, with a multitude of pores and voids clearly visible within the structure.

In Fig. 9, SEM images of geopolymers containing cork waste are reported. In particular, the cork waste is visible within the geopolymer matrix (purple rectangle) without affecting the peculiar geopolymer gel morphology, as already seen by XRD and FT-IR analysis. Within the yellow rectangle, the characteristic microstructure of the geopolymer is evident. In addition, the presence of crack deflections (red rectangle) is attributed to exposure to air and excessive water penetration due to the presence of cork waste. Pores are also clearly visible, as indicated by the white arrow.

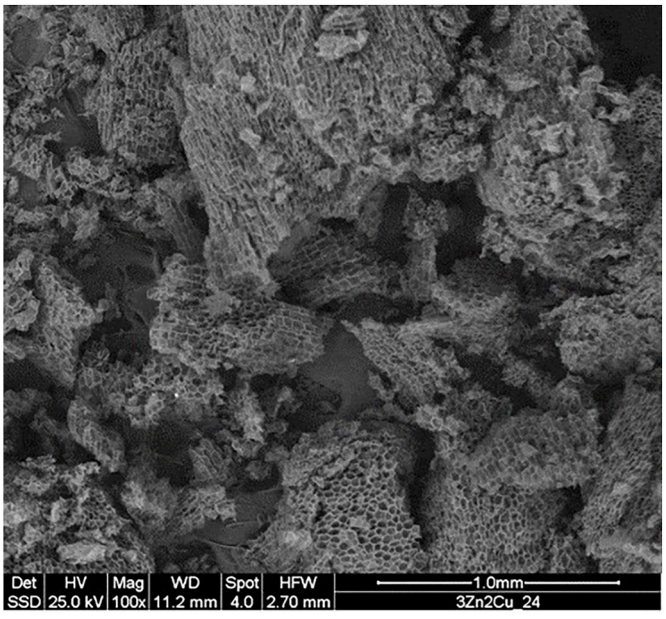

Fig. 8. Scanning Electron Microscopy (SEM) image, backscattered detector, of the as-received cork waste dust.

In Fig. 10, the focus shifts to samples containing 10 wt% cork, added before and after the alkaline activation. In the GP-10CW sample, unreacted cork is observed (purple rectangle), accompanied by crack deflections (red rectangle) and pull-outs (green rectangle). Meanwhile, the 90GP0-10CW sample shows a notable abundance of unreacted cork sites (purple rectangle) and visible pores (white arrow).

After treating the samples with acids, we performed SEM analysis to examine the effect on their microstructure. In order to identify specific areas for investigation, we used phenolphthalein 1 % solution to determine the extent and locations of acid penetration. In Fig. 11, it is evident that the pores (white rectangle) suffered damage upon exposure to the H_2SO_4 [53]. In addition, the H_2SO_4 caused structural degradation resulting in the formation of distinct grooves (black arrow). These grooves, resulting from sulfuric acid exposure, should not be confused with crack deflections (red rectangle). This distinction is clearly seen in Fig. 11c. Importantly, the cork material (purple rectangle) remained remarkably inert to this type of chemical attack.

In the concluding phase, the infiltration of sulphur into the microstructure of the geopolymer matrix was investigated by EDS. Fig. 12 shows the SEM image of the 90GP0-10CW sample, supplemented by EDS data from four distinct areas, spanning from the innermost to the outermost regions. Notably, the analysis shows a decrease in sulphur penetration as one approaches the core of the geopolymer. This observation suggests that the interior of the geopolymer has experienced a comparatively milder chemical attack, which would be expected to preserve its structural performance (see next paragraph).

The Na profile (not reported here) is the opposite of the sulphur profile, demonstrating the ionic exchange with H^+ as expected from previous studies and modeling [54].

3.7. Mechanical properties

Compressive strength tests were performed on all the geopolymer samples after 28 days of ageing. Fig. 13 shows their compressive strength before the exposure to acid attack. The introduction of waste cork reduces the mechanical properties while making the material lighter. Geopolymers with cork added after alkali activation are

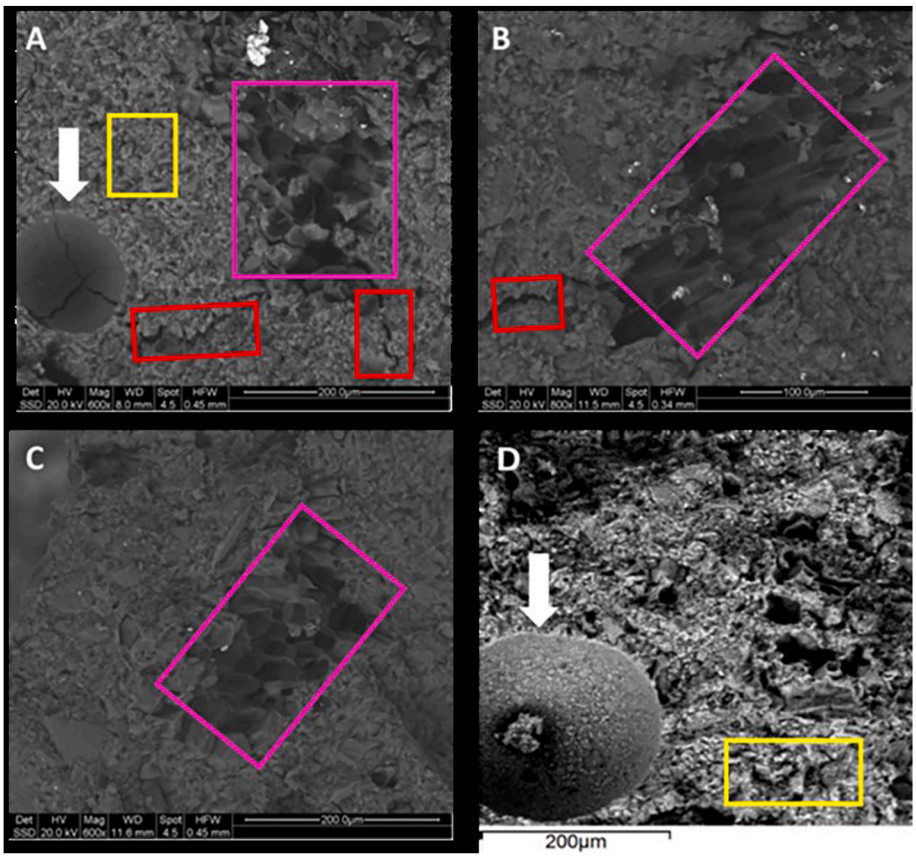

Fig. 9. Scanning Electron Microscopy images taken at low magnification of A) GP-2CW; B) GP-5CW C) GP-10CW; D) 90 GP-10CW, before acid attack.

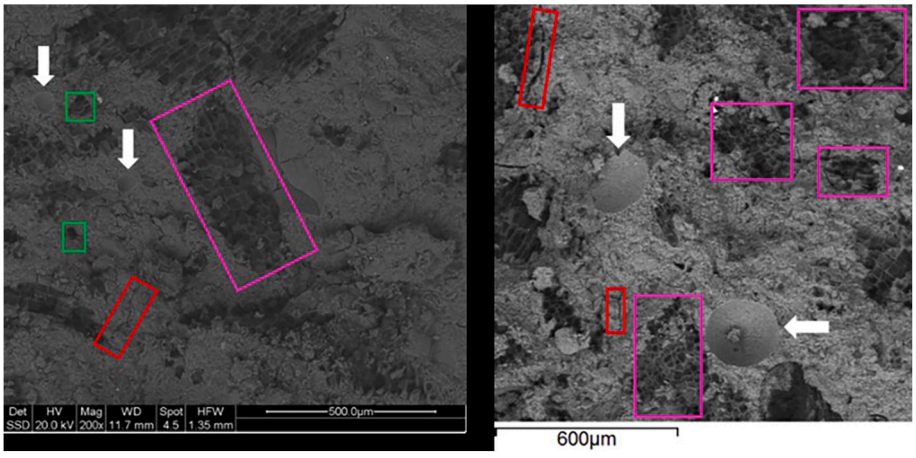

Fig. 10. Focus on sample GP-10CW (left) and 90 GP-10CW (right), before acid attack.

exceptionally light and porous, resulting in significantly reduced mechanical strength. The low strength is primarily due to the presence of cork; when added after alkali activation, it assumes a disordered arrangement within the geopolymer network and absorbs excess water from the geopolymer paste. Remarkably, this does not interfere with the geopolymerization process, as previously observed. This phenomenon can be observed even with small amounts of cork, as in the case of 95GP0-5CW.

After testing the geopolymers before and after immersion in acids, the results were compared (Figs. 14 and 15). Mechanical properties remained fairly consistent when extracted from low concentration acid solutions. However, at higher concentrations, the results differed.

In particular, Fig. 15 shows that the two composites containing cork after alkali activation, namely 95GP0-5CW and 90GP0-10CW, were omitted from the test. This omission was not due to their inability to withstand the acid attack, as the weight loss was not excessive. Rather, the cork had absorbed so much acid solution that it disintegrated under minimal pressure. In contrast, the other samples, GP-2CW, GP-5CW, GP-7CW, and GP-10CW, were tested and showed lower values. The difference in performance between these two series of formulations is primarily due to the ability of the cork to absorb a significant amount of acid solution due to its high porosity and increased diffusivity within the bulk sample.

As a final remark on the results of the mechanical resistance after the

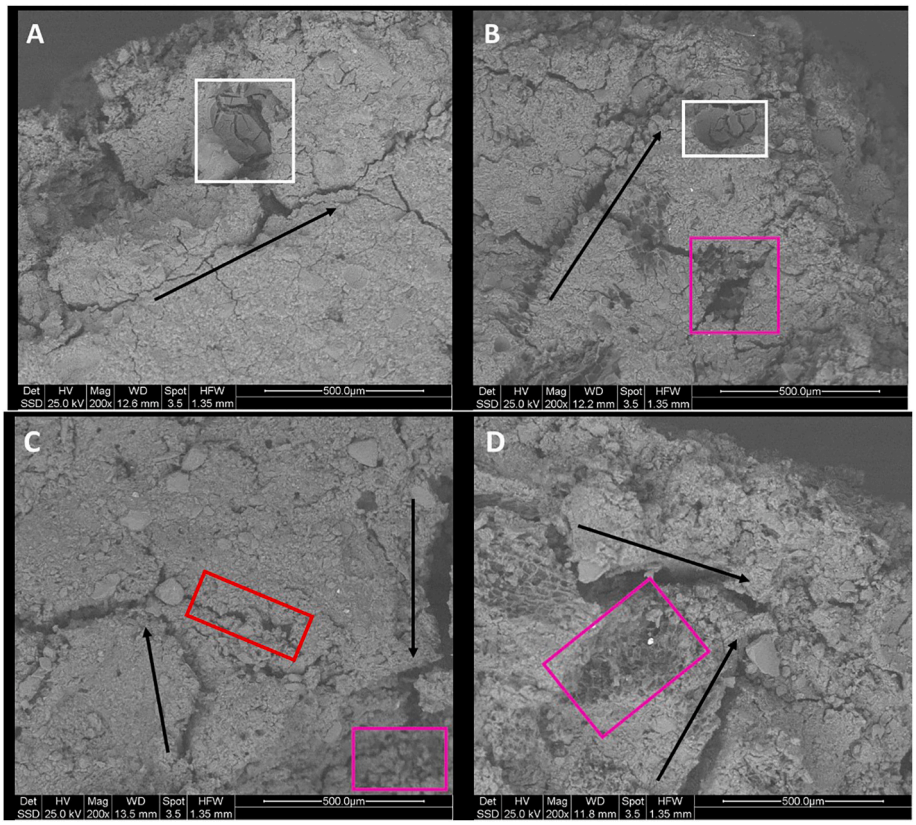

Fig. 11. Scanning Electron Microscopy images taken at low magnification after acid attack of A) GP-2CW; B) GP-5CW C) 90 GP-10CW inner part; D) 90 GP-10CW surface.

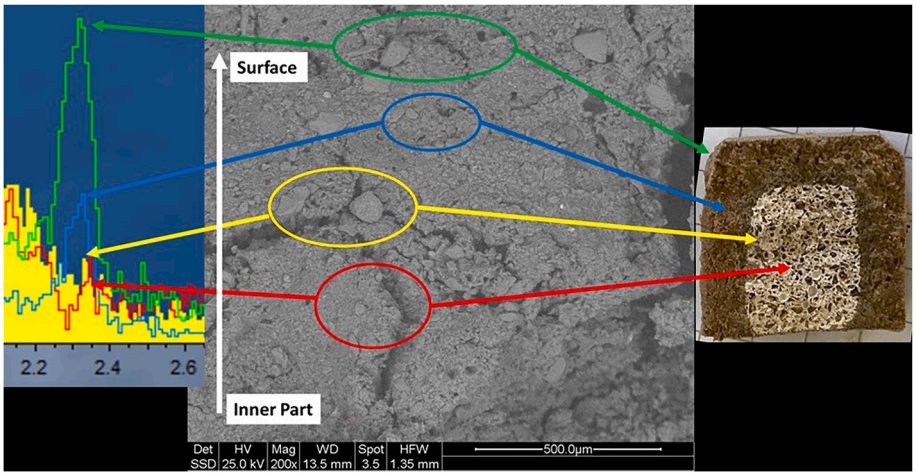

Fig. 12. SEM and EDS analyses of sample 90GP0-10CW with an enlargement around the peak of sulphur 2.3 keV to evidence the penetration of sulphate ions, as visualised via the phenolphthalein test.

acid immersion of the samples, we can assess that the ionic exchange of H^+ or H_3O^+ for Na^+ is indeed the most aggressive process [55,56]. The two acids have the same normality, that is to say that they have the same concentration of H^+ and produce the same reduction in mechanical performance, regardless the type of anion, either sulphate or nitrate. The permeation of the acid with the composite volume is also proportional to the porosity as well as the diffusivity, indicating that the microstructure plays a relevant role [57]. The presence of cork dust as a filler favours the penetration of the acid solution and accelerates the degradation of the composite.

4. Conclusions

With the aim of increasing the sustainability of building materials, a possible insulating composite material is formulated with a metakaolin-based geopolymer, as the matrix, to which the as-received cork dust by-product was added as filler or lightweight aggregate. The composite material can be prepared either by mixing the cork dust with the dry metakaolin or by adding the cork to the MK-based geopolymer paste already mixed with the alkaline activator solutions. The two mixing procedures result in two different types of composites, both hardened at room temperature, which differs mainly in the microstructure rather

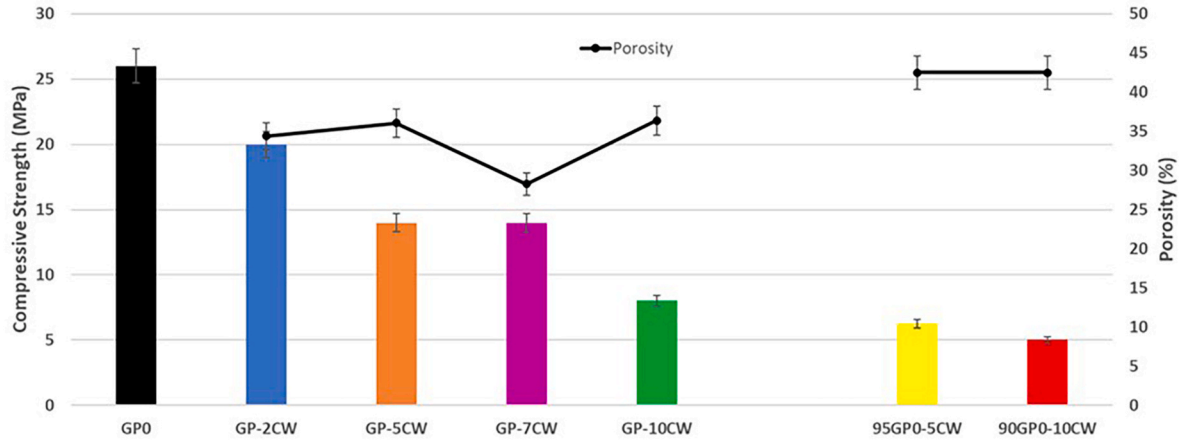

Fig. 13. Compressive strength of all samples (28 days of ageing) before acid attack.

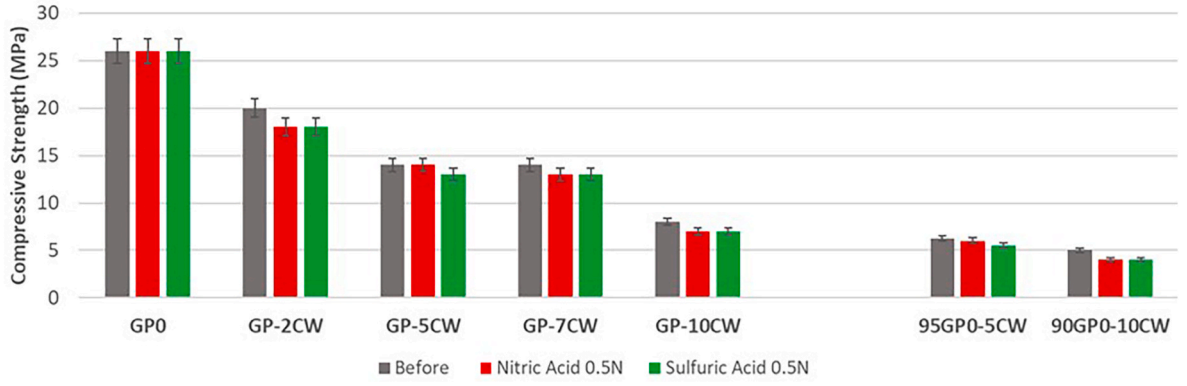

Fig. 14. Compressive strength (MPa) of all the samples before and after acid attack at low concentration (0.5 N).

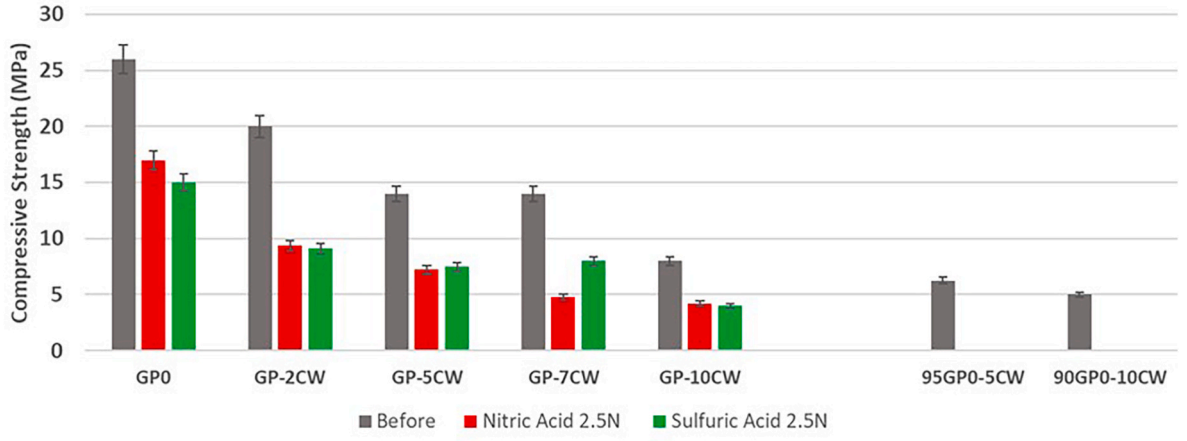

Fig. 15. Compressive strength (MPa) of all the samples before and after acid attack at high concentration (2.5 N).

than in the degree of reticulation of the geopolymer matrix. The final performance of the composite was tested starting from its stability in water, acid, and under compression. In the acidic environment, it was shown that the degradation mechanism starts from the exchange of H^+ for Na^+, such sodium balancing the charges of the [AlO_4] tetrahedra, when it is absent, makes the originally stable non-bridging oxygen active again, promoting hydrolytic reactions. Newly formed hydroxyls (silanol species) cause further swelling of the structure. The results indicate that a control of the microstructure, in terms of density and porosity, is necessary to achieve the adequate performance of the hardened composite. The control on the microstructure can be obtained by the dosage of the cork dust and the correct mixing procedure.

Declaration of competing interest

The authors declare that they have no known competing financial interests or personal relationships that could have appeared to influence the work reported in this paper.

Acknowledgements

Authors are particularly grateful for metakaolin supply to Sophie Maraninchi, Product Manager Refractory, Abrasives and Constructions Business Area, Imerys, France, and Paola Morsiani, Sales Manager, Performance Minerals EMEA/Ceramics, Imerys Ceramics Italy. Authors express their gratitude to Dr. Mirko Braga and Pasquale Pansini, Ingessil, Montorio, Verona, Italy, for supplying the sodium silicate solution and to Italsughero of F.lli Correggi S.r.l. (Montecchio Emilia—RE, Italy) for the supply of the cork waste.

References

[1] A. Raut, R.J. Singh, A. Murmu, K.A. Khan, Evaluation of thermal and energy consumption behavior of novel foamed copper slag based geopolymer masonry blocks, Ceram. Int. 48 (9) (2022) 12098–12111.
[2] F. Ghonjizade-Samani, L. Haurie, R. Malet, V. Realinho, The components' roles in thermal stability and flammability of cork powder, Materials 16 (10) (2023) 3829.
[3] J.B. Engel, C.L. Luchese, I.C. Tessaro, Characterization techniques comparison towards a better understanding of different cork-based stoppers types, J. Food Eng. 328 (2022) 111063.
[4] G. Luciano, A. Vignali, M. Vignolo, R. Utzeri, F. Bertini, S. Iannace, Biocomposite foams with multimodal cellular structures based on cork granulates and microwave processed egg white proteins, Materials 16 (8) (2023) 3063.
[5] R.M. Novais, L. Senff, J. Carvalheiras, J.A. Labrincha, Bi-layered porous/cork-containing waste-based inorganic polymer composites: innovative material towards green buildings, Appl. Sci. 10 (9) (2020) 2995.
[6] J. Li, A. Zhang, S. Zhang, Q. Gao, W. Zhang, J. Li, Larch tannin-based rigid phenolic foam with high compressive strength, low friability, and low thermal conductivity reinforced by cork powder, Composites, Part B 156 (2019) 368–377.
[7] N. Gama, A. Ferreira, D. Evtuguin, A. Barros-Timmons, Modified cork/SEBS composites for 3D printed elastomers, Polym. Adv. Technol. 33 (6) (2022), 1881-189.
[8] F. Ben Abdallah, R. Ben Cheikh, M. Baklouti, Z. Denchev, A.M. Cunha, Characterization of composite materials based on PP-cork blends, J. Reinforc. Plast. Compos. 25 (14) (2006) 1499–1506.
[9] N. Gaibor, R. Mateus, D. Leitão, N. Cristelo, T. Miranda, E.N.B. Pereira, V.M.C. F. Cunha, Sustainability assessment of half-sandwich panels based on alkali-activated ceramic/slag wastes cement versus conventional building solutions, J. Clean. Prod. 389 (2023) 136108.
[10] G. Dal Poggetto, R. Marchetti, I. Lancellotti, C. Leonelli, L. Barbieri, Waste cork in metakaolin–geopolymer matrix: physico-mechanical characterization, Appl. Sci. 13 (3) (2023) 1804.
[11] F. Barreca, A. Martinez Gabarron, J.A. Flores Yepes, J.J. Pastor Pérez, Innovative use of giant reed and cork residues for panels of buildings in Mediterranean area, Resour. Conserv. Recycl. 140 (2019) 259–266.
[12] V. Van Tran, D. Park, Y.-C. Lee, Indoor air pollution, related human diseases, and recent trends in the control and improvement of indoor air quality, Int. J. Environ. Res. Publ. Health 17 (8) (2020) 2927.
[13] S. Dawcznski, M. Gorski, R. Krzywon, Granulated cork as a component of geopolymer —preliminary studies, Ann. Wars. Univ. Life Sci.-SGGW For. Wood Technol. 94 (2016) 124–128.
[14] A. Sudagar, S. Andrejkovicova, C. Patinha, A. Velosa, A. McAdam, E. Ferreira da Silva, F. Rocha, A novel study on the influence of cork waste residue on metakaolin-zeolite based geopolymers, Appl. Clay Sci. 152 (2018) 196–210.
[15] R.M. Novais, M. Saeli, A.P.F. Caetano, M.P. Seabra, J.A. Labrincha, K.P. Surendran, R.C. Pullar, Pyrolysed cork-geopolymer composites: a novel and sustainable EMI shielding building material, Constr. Build. Matls. 229 (2019) 116930.
[16] R.M. Novais, J. Carvalheiras, L. Senff, A.M. Lacasta, I.R. Cantalapiedra, J. Giro-Paloma, M.P. Seabra, J.A. Labrincha, Multifunctional cork—alkali-activated fly ash composites: a sustainable material to enhance buildings' energy and acoustic performance, Energy Build. 210 (2020) 109739.
[17] R.M. Novais, L. Senff, J. Carvalheiras, M.P. Seabra, R.C. Pullar, J.A. Labrincha, Sustainable and efficient cork—inorganic polymer composites: an innovative and eco-friendly approach to produce ultra-lightweight and low thermal conductivity materials, Cem. Concr. Compos. 97 (2019) 107–117.
[18] R.M. Novais, L. Senff, J. Carvalheiras, A.M. Lacasta, I.R. Cantalapiedra, J. A. Labrincha, Simple and effective route to tailor the thermal, acoustic and hygrothermal properties of cork-containing waste derived inorganic polymer composites, J. Build. Eng. 42 (2021) 102501.
[19] N. Lakreb, U. Şen, E. Toussaint, S. Amziane, E. Djakab, H. Pereira, Physical properties and thermal conductivity of cork-based sandwich panels for building insulation, Constr. Build. Matls. 368 (2023) 130420.
[20] I. Romero-Ocaña, S.I. Molina, Cork photocurable resin composite for stereolithography (SLA): influence of cork particle size on mechanical and thermal properties, Addit. Manuf. 51 (2022) 102586.
[21] R. Carvalho, M. Fernandes, R. Fangueiro, The influence of cork on the thermal insulation properties of home textiles, Procedia Eng. 200 (2017) 252–259.
[22] D.K. Panesar, B. Shindman, The mechanical, transport and thermal properties of mortar and concrete containing waste cork, Cem. Concr. Compos. 34 (9) (2012) 982–992.
[23] E.M. Fernandes, V.M. Correlo, J.F. Mano, R.L. Reis, Cork–polymer biocomposites: mechanical, structural and thermal properties, Matls & Design 82 (2015) 282–289.
[24] B. Malchiodi, R. Marchetti, L. Barbieri, P. Pozzi, Recovery of cork manufacturing waste within mortar and polyurethane: feasibility of use and physical, mechanical, thermal insulating properties of the final green composite construction materials, Appl. Sci. 12 (2022) 3844.
[25] G. Dal Poggetto, M. Catauro, G. Crescente, C. Leonelli, Efficient addition of waste glass in MK-based geopolymers: microstructure, antibacterial and cytotoxicity investigation, Polymers 13 (2021) 1493.
[26] G. Dal Poggetto, A. D'Angelo, M. Catauro, L. Barbieri, C. Leonelli, Recycling of waste corundum abrasive powder in MK-based geopolymers, Polymers 14 (2022) 2173.
[27] I. Lancellotti, M. Catauro, C. Ponzoni, F. Bollino, C. Leonelli, Inorganic polymers from alkali activation of metakaolin: effect of setting and curing on structure, J. Solid State Chem. 200 (2013) 341–348.
[28] M. Zhang, H. Guo, T. El-Korchi, G. Zhang, M. Tao, Experimental feasibility study of geopolymer as the next-generation soil stabiliser, Constr. Build. Matls 47 (2013) 1468–1478.
[29] C. Ferone, B. Liguori, I. Capasso, F. Colangelo, R. Cioffi, E. Cappelletto, R. Di Maggio, Thermally treated clay sediments as geopolymeric feedstock, Appl. Clay Sci. 107 (2015) 195–204.
[30] Z.-T. Chang, X.-J. Song, R. Munn, M. Marosszeky, Using limestone aggregates and different cements for enhancing resistance of concrete to sulphuric acid attack, Cement Concr. Res. 35 (8) (2005) 1486–1494.
[31] F. Škvára, V. Šmilauer, P. Hlaváček, L. Kopecký, Z. Cílová, A weak alkali bond in (N, K)–A–S–H gels: evidence from leaching and modelling, Ceramics 56 (4) (2012) 374–382.
[32] U. Rattanasak, P. Chindaprasirt, Influence of NaOH solution on the synthesis of fly ash geopolymer, Miner. Eng. 22 (2009) 1073–1078.
[33] F.G.M. Aredes, T.M.B. Campos, J.P.B. MacHado, K.K. Sakane, G.P. Thim, D. D. Brunelli, Effect of cure temperature on the formation of metakaolinite-based geopolymer, Ceram. Int. 41 (6) (2015) 7302–7311.
[34] R. Müller, H. Behrens, B. Agea-Blanco, S. Reinsch, T. Wirth, Foaming species and trapping mechanisms in barium silicate glass sealants, Adv. Engineer. Matls 24 (6) (2022) 2100445.
[35] P.L. King, P.F. Mcmillan, G.M. Moore, Infrared spectroscopy of silicate glasses with application to natural systems, Infrared Spectrosc. Geochem. Explor. Geochem. Remote Sens. 33 (2004) 93–133.
[36] F. Miyaji, H.-M. Kim, S. Handa, T. Kokubo, T. Nakamura, Bonelike apatite coating on organic polymers: novel nucleation process using sodium silicate solution, Biomaterials 20 (10) (1999) 913–919.
[37] J. Lao, X. Dieudonné, M. Benbakkar, É. Jallot, Bioactive glass coating on gelatin scaffolds at ambient temperature: easy route to make polymer scaffolds become bioactive, J. Mater. Sci. 52 (2017) 9129.
[38] G.K. Priya, P. Padmaja, K.G.K. Warrier, A.D. Damodaran, G. Aruldhas, Dehydroxilation and high temperature phase formation in sol-gel boehmite characterized by Fourier transform infrared spectroscopy, J. Mater. Sci. Lett. 16 (1997) 1584–1587.
[39] D. Panias, I.P. Giannopoulou, T. Perraki, Effect of synthesis parameters on the mechanical properties of fly ash-based geopolymers, Colloids Surf. A Physicochem. Eng. Asp. 301 (2007) 246–254.
[40] G. Dal Poggetto, A. D'Angelo, I. Blanco, S. Piccolella, C. Leonelli, M. Catauro, Thermal analysis, and evaluation of the antibacterial activity of a MK-geopolymer mortar using glass waste as fine aggregate, Polymers 13 (2021) 2970.
[41] P. Makreski, G. Jovanovski, B. Kaitner, T. Stafilov, B. Boev, D. Cibrev, Minerals from Macedonia. X. Separation and identification of some oxide minerals by FT-IR spectroscopy, AAS, AES-ICP and powder XRD, Neues Jahrbuch Mineral. Abhand. 180 (2004) 215–243.
[42] B. Kalidasan, A. Pandey, S. Shahabuddin, M. George, K. Sharma, M. Samykano, V. Tyagi, R. Saidur, Synthesis and characterization of conducting Polyaniline@ cobalt-Paraffin wax nanocomposite as nano-phase change material: enhanced thermophysical properties, Renew. Energy 173 (2021) 1057–1069.
[43] T. Van Oosten, PUR Facts: Conservation of Polyurethane Foam in Art and Design, Amsterdam University Press, Amsterdam, The Netherlands, 2011.
[44] J. Temuujin, A. Minjigmaa, W. Rickard, M. Lee, I. Williams, A. Van Riessen, Preparation of metakaolin based geopolymer coatings on metal substrates as thermal barriers, Appl. Clay Sci. 46 (2009) 265–270.
[45] J.L. Provis, J.S. J Van Deventer, Geopolymers: Structure, Processing, Properties and Industrial Applications, Woodhead Publishing, Cambridge, UK, 2009.
[46] A.P. Poeiras, M.E. Silva, B. Günther, C. Vogel, P. Surovy, N. de Almeida Ribeiro, Cork influenced by a specific water regime—macro and microstructure characterization: the first approach, Wood Sci. Technol. 55 (2021) 1653–1672.
[47] E. Papa, E. Landi, F. Miccio, V. Medri, K_2O-metakaolin-based geopolymer foams: production, porosity characterization and permeability test, Materials 15 (2022) 1008.
[48] A. Allahverdi, F. Škvára, Nitric acid attack on hardened paste of geopolymeric cements Part I, Ceramics 45 (3) (2001) 81–88.
[49] A. Allahverdi, F. Škvára, Nitric acid attack on hardened paste of geopolymeric cements Part II, Ceramics 45 (4) (2001) 143–149.
[50] A. Allahverdi, F. Škvára, Sulphuric acid attack on hardened paste of geopolymer cements Part I: mechanism of corrosion at relatively high concentrations, Ceramics 49 (4) (2005) 225–229.
[51] P. Duxson, J.L. Provis, G.C. Lukey, S.W. Mallicoat, W.M. Kriven, J.S.J. van Deventer, Understanding the relationship between geopolymer composition, microstructure and mechanical properties, Colloids Surf. A Physicochem. Eng. Asp. 269 (2005) 47–58.

[52] H. Pereira, Cork: Biology, Production and Uses, first ed., Elsevier, Amsterdam, The Netherlands, 2007.
[53] G.J.G. Gluth, C. Grengg, N. Ukrainczyk, F. Mittermayr, M. Dietzel, Acid resistance of alkali-activated materials: recent advances and research needs, RILEM Technical Letters 7 (2022) 58–67.
[54] H. Wan, L. Yuan, Y. Zhang, Insight into the leaching of sodium alumino-silicate hydrate (N-A-S-H) gel: a molecular dynamics study, Front. Mater. Sec. Computational Materials Science 7 (2020).
[55] N. Ukrainczyk, O. Vogt, Geopolymer leaching in water and acetic acid, RILEM Tech. Lett. 5 (2020) 163–173.
[56] O. Vogt, C. Ballschmiede, N. Ukrainczyk, E. Koenders, Evaluation of sulfuric acid-induced degradation of potassium silicate activated metakaolin geopolymers by semi-quantitative SEM-EDS analysis, Materials 13 (2020) 4522.
[57] E. Rozière, A. Loukili, Performance-based assessment of concrete resistance to leaching, Cem. Concr. Compos. 33 (2011) 451–456.